DISTRIBUTION OF THE ENERGETIC PARTICLE "INJECTION" EVENTS ALONG THE RADIATION BELT SLOPE.

L. Lazutin
Polar Geophysical Institute, Apatity, Murmansk Region, 184200 Russia,

A.Korth
Max-Planck-Institute fur Aeronomie, D-37191 Katlenburg-Lindau, Germany

Abstract. Dispersionless increases of the energetic electrons and ions usually referred as injection are known as an important process of the onset or intensification of magnetospheric substorm active phase. The CRRES satellite nearly half of each orbit (5-6 hours) was moving through the outer radiation belt and therefore is favorable for the statistical study of the injection events. Statistical distribution of the injections versus local time, radial distance or L-value have been published. But as the magnetosphere is changing considerably during substorms, it is important to know the relative position of the injections comparative to the main magnetospheric regions, such as radiation belt or magnetotail. For this purpose we introduce a relative distance (RD) index as a ratio of the particle intensity at the maximum of the radiation belt to the intensity at the belt slope at the moment of the observation. The results shown, that injection region is superimposed with the outer radiation belt. inside. Their number and averaged injection amplitude are decreasing toward the isotropic boundary of 20-50 keV electrons.

1. Introduction

Dispersionless increases of the energetic electrons and ions are observed simultaneously with the onset or the intensification of magnetospheric substorm simultaneously with magnetic field dipolarization, formation of the substorm current wedge and other important processes of the active phase. Such increases are usually referred as an "injection" events [*Mauk and McIlwain*, 1974, *McIlwain*, 1974, *Friedel et al*., 1994]. The initial conception of this term suggests that enhanced particles have been transported, or injected from the magnetotail, which is not so evident now. To found out, whether energetic electrons and protons are locally accelerated or transported from the tail, it is important to know relative position of the injection events.

Injections are commonly observed at geosinchronous region of the midnight sector, at the radial distances of 4.5-9 Re [*Friedel et al.*1996, *Perry et al*., 1996]. In this sector of the magnetosphere the inner edge of the plasmasheet is located, and occasionally trapping boundary may be found as deep as that, which leave indistinct where the substorm main active processes such as the breakups and intensifications are taking place.

The CRRES satellite nearly half of each orbit period (5-6 hours) have been moving through the outer radiation belt, from maximum toward the boundary and back to the Earth and therefore is favorable for the statistical study of the injection events.

In present paper we are using energetic particle measurements on board of a satellite CRRES for the statistical study of the injection relative position (or more accurately - the position of the satellite at the moment of the observation) in the radiation belt. We introduce a relative distance (RD) of the injection from the radiation belt maximum as a ratio of the particle intensity at the maximum of the radiation belt to the minimum intensity at the slope of the belt just before the intensity increase. More than 40 injection events have been inspected and their position relative to the outer radiation belt have been discussed.

2. Data Analysis

Energetic electrons and ions have been measured on board os CRRES by energetic particle spectrometer EPAS [*Korth et al*., 1992] . We did not make special data selection for this analysis. CRRES orbits have been chosen for different substorm studies and we are using accumulated material - 42 injection events from 25 CRRES orbits. Most of them are accompanied by magnetic field dipolarization, Pi2 pulsations, magnetic and other signatures of the substorm breakup or intensification.

2.1. Relative position: a definition

To identify the position of the satellite in the radiation belt during the injection event one need specify the reference scale. It might be based on the rate of the intensity decrease on the slope of the radiation belt weighted against the radiation belt maximum.

This point - the intensity maximum of the outer radiation

belt (RBM)- is present on all CRRES orbits. Comparing the particle intensity right before the injection increase with nearest maximum value, we will have the *relative distance* (RD) from the maximum, or *relative* satellite *position* at the moment of the injection.
The EPAS particle detectors have 12 differential channels for ions and 14 for the electrons therefore there are 26 candidates for the RD index. Of cause, not all the channels can be used for the reference scale: high energy channels on the large part of the radiation belt slope have counting rate below the sensitivity level, whereas at the low energy channels the presence of the energetic particles accelerated in the previous activity may conceal the real radiation belt intensity. But the majority of the channels can be used as a source of the RD index. We have used several reference scales based on different data channels and the results, which will be described below, were approximately the same with a different RD.
Figure 1 illustrates a RD definition procedure. It shows typical change of the particle intensity during the orbit, but instead of the time scale or distance relative position is used for the x-axis.

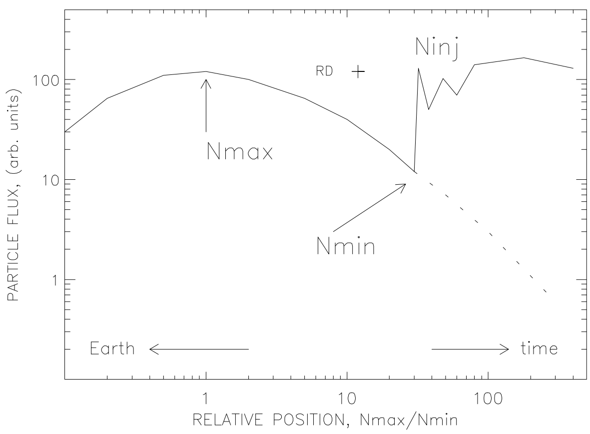

Figure 1. A definition of the injection relative position

We will refer as RDe4 the relative distance based on electron channel number 4 (49.5-59 keV). RDe4 is equal to the ratio Ne4max/Ne4min of differential electron intensity at the RBM and at the intensity minimum before the injection increase e4inj. Similarly RDe8 and RDp8 were calculated using 94.5-112 keV electron channel and 254-335 keV proton channel.

2.2. Distribution of the relative position of the injection events.

Figure 2 presents a distribution of the injection intensity (Ninj - Nmin) versus RDe4 for individual events and intensity averaged for several RD intervals (solid line). At the bottom panel the histogram of distribution of the injection events along the radiation belt slope is given. The arrow indicates the position of the isotropic radiation belt boundary of > 30 keV electrons estimated from the measurements on CRRES orbits, where this boundary was registered.
One can see, that most of the events are located inside the boundary of the radiation belt, approximately uniformly

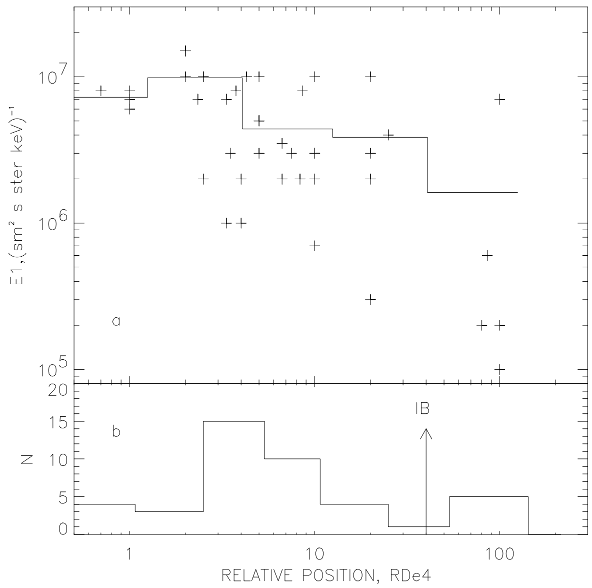

Figure 2 Energetic electron (21.5-31.5 keV) increase intensity versus relative position in the radiation belt. Solid line shows an avereage flux intensity. Bottom panel - distribution of the injection events versus relative position. Arrow indicate isotropic boundary relative position.

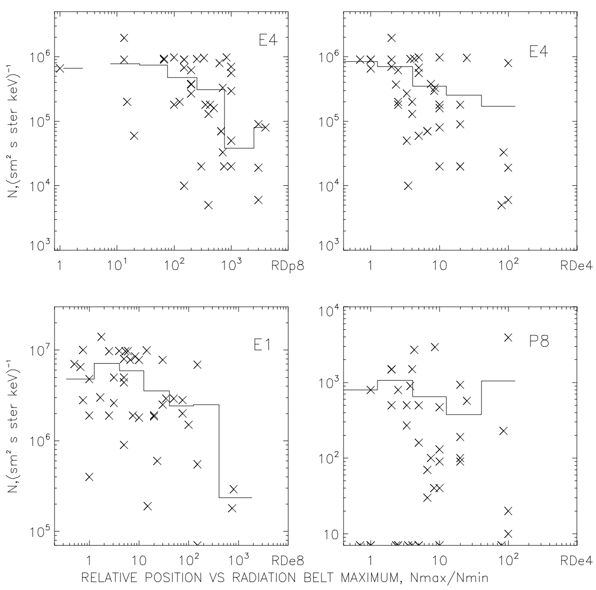

Figure 3 Increase intensity versus relative distance from the radiation belt maximum for E4, E1 and P8 channels versus RDp8, Rde4 and Rde8 relative position scales.

along the slope of the belt, some of them right at the maximum (RD=1). They are not concentrated near the radiation belt boundary, moreover, toward the lower part of the slope number of the registered injections are decreasing,.

The second important effect is a decrease of the injection intensity toward the boundary of the radiation belt. The maximum of enhanced particle flux is located close to the radiation belt maximum, and the difference with the boundary region is considerable, taking into account the intensity logarithmic scale. Of cause, the dispersion of the individual amplitudes is considerable.

Both effects can be seen in other energy channels, as shown by Figure 3. In two panels at the right side the same RDe4 index was used for P8 and E4 increases, while at the left panels we use RDe8 and RDp8 for the reference scale. Energetic protons maximum is located closer to the Earth and intensity decreases faster to the background level, therefore most of the points are located at the lower part of proton belt slope. Other three panels show that average injection intensity and number density have a maximum well inside the radiation belt.

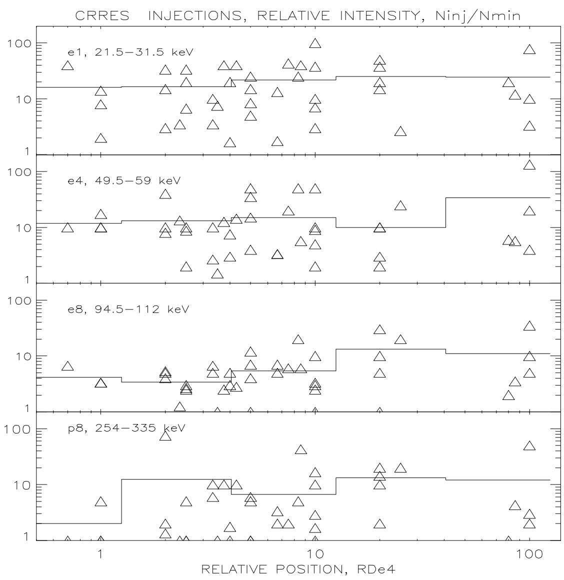

Figure 4 Distribution of the relative increase amplitude, defined as (Ninj-Nmin)/Nmin for different electron and ion energies versus relative position RDe4.

Figure 4 shows results for the relative intensity increases, calculated as (Imax - Imin)/Imin. Distribution of the relative amplitudes is nearly uniform over the radiation belt slope, the higher initial flux gave higher injection amplitude.

Figure 5 present results of the comparison of the injection intensity for two electron and two ion channels. Good correlation between two electron channels is not surprising, electrons are accelerated in a wide energy range. The dispersion of points shows, that energy spectrum of the accelerated flux differs considerably from one case to another. Good correlation of the electron increases with the energetic ions increase suggests, that mechanism of the acceleration is similar or the same for

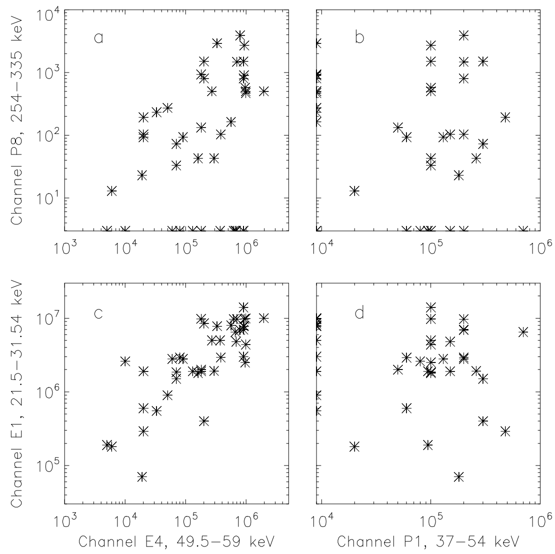

Figure 5 Comparision of the amplitudes of the intensity increases of several electron and ion channels. a) – P8 versus E4, b) – P8 versus P1, c) – E1 versus E4, d) – E1 versus P1

electrons and ions, although there are some cases, when the proton increase is small or absent. The poorest correlation is observed between low energy and high energy protons. In many cases during injections a decrease in P1 channel was registered.

3. Conclusion

The relative intensity method contains certain errors. The intensity on the radiation belt maximum is changing considerably from one orbit to another, the trajectories of the satellite are different, the results also depend on the history of previous magnetospheric activity. Certainly there are better procedures for definition of the satellite position in the trapping region, such as local magnetic field configuration. But the possible errors of the RD method does not influence the main results of this study: (1) injection events were recorded by CRRES distributed along the radiation belt slope from the intensity maximum to the boundary, (2) majority of the events situated well inside the isotropic boundary without concentration near the boundary, (3) average intensity of the increased flux is decreased toward the radiation belt boundary.

These conclusions agreed with the current disruption model of the magnetospheric substorm onset [Lui et al, 1990, 1992] and with resistive shear flow- ballooning instability model of substorm intensifications [Samson et al, 1996], which suggests that the instability region is located at the inner edge of the plasmasheet. In the midnight sector of the disturbed magnetosphere inner edge of the plasmasheet moves earthward and overlapping with considerable part of the radiation belt slope.

References

Birn, J. and et al., Plasma and energetic particle properties of dispersionless substorm injections at geosynchronous orbit. *Proc.of the Third Int.Con.on Subs.* 3:321-326, 1996.

Friedel, R.H.W., Korth, A., Reeves, G.D. and Belian, R. Origin of energetic particle injections at substorm onset as measured by the CRRES spececraft between 4 and 7 Re and Los Alamos geostationary satellites. *Proc.of the Second Int.Con.on Subs.* 2:571-576, 1994.

Friedel, R.H.W.,and Korth, A. D Substorm onset observed by CRRES: constraints on energetic electron source *Proc.of the Third Int.Con.on Subs.* 3:473-479, 1996

Korth, A., Kremser, G., Wilken, B., Guttler, W., Ullaiand, S.L. and Koga, R. Electron and proton wide-angle spectrometer (EPAS) on the CRRES spacecraft. *J.of Spacecraft and Rockets.* 29:609-614, 1992.

Lui, A.T.Y., Lopez, R.E., Anderson, B.J., et al. Current disruptions in the near-Earth neutral sheet region. *J.Geophys.Res,* 97:1461-1480, 1992.

Lui, A.T.Y., Lopez, R.E., Krimigis, S.M., McEntire, R.W., Zanetti, L.J. and Potemra, T.A. A case study of magnetotail current sheet disruption and diversion. *Geophys.Res.Lett*. 15:721-724, 1988.

Lui, A.T.Y., Mankofsky, A., Chang, C.-L., Papadopulos, K. and Wu, C.S. A current disruption mechanism in the neutral sheet: A possible trigger for substorm expansions. *Geophys.Res.Lett*. 17, N 6:745-748, 1990.

Mauk, B.H. and McIlwain, C.E. Correlation of Kp with the substorm injected plasma boundary. *J.Geophys.Res*. 79, N 22:3193-3196, 1974.

McIlwain, C.E. Substorm injection boundaries. *In: Magnetospheric physics, edited by McCormac, B.M. Dordrecht-Holland/Boston-U.S.A.: D.Reidel Pub. Comp.,* 1974, p. 143-154.

Perry, C.H. and et al., Statistical survey of dispersionless substrom injections observed by the CREES MICS ion spectrometer. *Proc.of the Third Int.Con.on Subs.* 3:567-572, 1996.

Samson, J.C., MacAulay, A.K., Rankin, R., Frycz, P., Voronkov, I. and Cogger, L.L. Substorm intensifications and resistive shear flow-ballooning instabilities in the near-Earth magnetotail. *Third International Conference on Substorms (ICS-3),Versailles,France,12-17 May 1996*,ESA SP-389. 3:399-404, 1996.

Published in: Substorms-4, edited by S. Kokubun and Y. Kamide, pp. 817-820, Terra, Tokyo, 1998